

# Hypoxia Promotes CEMP1 Expression and Induces Cementoblastic Differentiation of Human Dental Stem Cells in an HIF-1-Dependent Manner

Hwajung Choi, PhD,<sup>1</sup> Hexiu Jin, MD, PhD,<sup>1</sup> Jin-Young Kim, MS,<sup>1</sup> Ki-Taek Lim, PhD,<sup>1,2</sup>  
Han-Wool Choung, DDS, MSD,<sup>1</sup> Joo-Young Park, DDS, PhD,<sup>1</sup>  
Jong Hoon Chung, PhD,<sup>2,\*</sup> and Pill-Hoon Choung, DDS, MSD, PhD<sup>1,\*</sup>

Cementum covering the tooth root provides attachment for the tooth proper to the surrounding alveolar bone via non-mineralized periodontal ligament (PDL). Cementum protein 1 (CEMP1) has been shown to induce a cementoblastic phenotype in cementoblast precursor cells of PDL. Oxygen availability is a critical signal for correct development of many tissues; however, its role in tooth root and periodontium development remains poorly understood. In this study, we demonstrated that reduced oxygen tension increased CEMP1 expression, mineral deposition, and alkaline phosphatase activity in human dental stem cells such as PDL stem cells and periapical follicular stem cells. Since an oxemic state is transduced by the transcription factor, hypoxia-inducible factor-1 (HIF-1), we performed experiments to determine whether this protein was responsible for the observed changes. We noted that when HIF-1 was activated by gene introduction or chemically, CEMP1 expression and mineralization increased. In contrast, when HIF-1 $\alpha$  was silenced, CEMP1 expression and mineralization did not increase *in vitro*. Furthermore, we showed for the first time that mouse tooth root and periodontium development occurs partly under hypoxic conditions, particularly at the apical part and latently at the PDL space *in vivo*. Desferrioxamine, an HIF-1 stimulator, enhances CEMP1 expression in the mouse PDL space, suggesting that hypoxia affects cementogenesis of PDL cells lining the surface of the developing tooth root in an HIF-1-dependent manner. These results suggest that HIF-1 activators may have the ability to stimulate regeneration of the tooth root and cementum formation.

## Introduction

**T**HE PERIODONTIUM, defined as tissues that support and house the dentition, comprises root cementum, periodontal ligament (PDL), and alveolar bone.<sup>1</sup> Cementum formation is critical for development of the periodontium and regeneration of periodontal tissues.<sup>2</sup> Cementum is a mineralized tissue which is produced by cementoblasts covering the roots of teeth that facilitates attachment of PDL to roots and surrounding alveolar bone.<sup>3,4</sup> Two main types of cementum are recognized: acellular extrinsic fiber cementum (AEFC) and cellular intrinsic fiber cementum. Acellular cementum consists of closely packed collagen fibers that originally form a part of the PDL and are, thus, considered extrinsic, and a mineralizing ground substance of noncollagenous proteins. This type of cementum is presumably a product of PDL cells. Cellular cementum covers the interradicular root dentin and the apical portion of the outer root surface. Cellular cementum is deposited by cementoblasts, progenitors of cementocytes, whenever they are enclosed by

mineralized cementum. These cementoblasts deposit a mineralizing matrix that is rich in intrinsic collagen fibrils and non-collagenous proteins directly onto the root surface, which mixes with the extrinsic collagen fibrils deposited earlier by PDL cells.<sup>4</sup>

Despite the important role that cementum plays in the reparative process after periodontal disease, very little is known about its progenitors, cementoblasts. Initially, cementum protein 1 (CEMP1) was isolated and characterized as a human cementoblastoma-derived protein<sup>5</sup> and *in situ* hybridization revealed that CEMP1 mRNA was expressed in the cementoblast cell layer lining the cementoid surface of cementum.<sup>6</sup> Transfection of the CEMP1 coding region (GenBank Accession No. NM\_001048212) into human gingival fibroblasts showed that CEMP1 promotes cell attachment and osteoblastic and/or cementoblastic cell differentiation.<sup>7,8</sup> Recently, it was found that purified human recombinant CEMP1 has strong affinity for hydroxyapatite and promotes octacalcium phosphate (OCP) crystal growth as a part of the biomineralization process.<sup>9</sup> OCP is presumed

<sup>1</sup>Department of Oral and Maxillofacial Surgery, Dental Research Institute, School of Dentistry, Seoul National University, Seoul, Korea.

<sup>2</sup>Department of Biosystems and Biomaterials Science and Engineering, Research Institute for Agriculture and Life Sciences, Seoul National University, Seoul, Korea.

\*Co-Corresponding authors.

to be a necessary precursor of biological apatites in hard tissue calcifications.<sup>9</sup> Furthermore, immunohistochemical staining of human periodontal tissue confirmed that the CEMP1 protein localized to cementoblast cells as well as to restricted PDL cell subpopulations (cementoblast precursors) in the PDL space (Supplementary Fig. S1; Supplementary Data are available online at [www.liebertpub.com/tea](http://www.liebertpub.com/tea)). These results strongly suggest that CEMP1 may regulate cementoblast differentiation during development and in the adult PDL space.

Oxygen is both a potent biochemical signaling molecule and a major gene regulator during an organism's development.<sup>10</sup> During development, oxygen participates in the intricate balance between cellular proliferation and commitment toward differentiation. Furthermore, oxygen concentration significantly influences the way in which cells remodel their environment, for example, matrix regulation.<sup>11,12</sup> The response to hypoxia is cell-type dependent, but oxygen affects critical cellular processes such as adhesion, proliferation, metabolism, apoptosis, growth factor expression, extracellular matrix secretion, and differentiation patterns.<sup>10,13–16</sup> Hence, oxygen affects cellular characteristics and tissue-remodeling processes, and may have the potential to direct cell fate.<sup>17–19</sup> The hypoxia-inducible factor (HIF) pathway is the central pathway for sensing and responding to changes in local oxygen availability in a wide variety of organisms.<sup>20</sup> HIF-1 $\alpha$  dimerizes with HIF-1 $\beta$  (ARNT) to form the HIF-1 transcription factor, and HIF-2 is similarly formed via the association of HIF-2 $\alpha$  and HIF-1 $\beta$ : Both HIF-1 and HIF-2 activate transcription. HIF-1 is known to play an important role in modulating cell fate, including osteogenic differentiation.<sup>20,21</sup> However, little is known about the role of hypoxia and HIFs in tooth development.

Human dental stem cells (DSCs) are recognized as a promising source for cell-based, autologous tissue regeneration.<sup>22,23</sup> Thus, understanding the cellular and molecular biology of these cell populations is the current focus of translational research. Accumulating evidence suggests that local oxygen tension is a critical modulator of mesenchymal cell growth and differentiation.<sup>17</sup> The purpose of this study was to investigate the effects of hypoxia on cementoblastic differentiation of human DSCs, including periapical follicular stem cells (PAFSCs) and periodontal ligament stem cells (PDLSCs). We hypothesized that hypoxia affects the differentiation potential of DSCs and tooth development. Here, we show for the first time that mouse tooth root and periodontium development occurs partly in a hypoxic state, particularly at the apical part and latently at the PDL space. In addition, we demonstrate that hypoxia stimulates CEMP1 expression, at least partly, via a pathway involving HIF-1 *in vitro* and that mice treated with desferrioxamine (DFO), a chemical inducer of HIF-1 protein, show an increase in CEMP1 expression during tooth root development *in vivo*. Our data indicate that hypoxia stimulates CEMP1 expression and enhances cementum formation in a developing tooth root in an HIF-1-dependent manner.

## Materials and Methods

### Primary cell culture from human dental tissue

Human third molars were collected from healthy young men (18–25 years) under the protocol approved by the in-

stitutional review board of Seoul National University Dental Hospital, Seoul, Korea (IRB Number 05004). Periapical follicles were separated from the root of the tooth germs at the root-forming stage, and they were aseptically dissected to obtain human PAFSCs. PDL tissues were separated from the surface of the root to obtain human PDLSCs. Separated tissues were digested in a solution of 3 mg/mL collagenase type I (Worthington Biochem, Freehold, NJ) and 4 mg/mL dispase (Boehringer, Mannheim, Germany) for 1 h at 37°C. Single-cell suspensions were obtained by passing the cells through a 40  $\mu$ m strainer (BD Labware, Franklin Lakes, NJ) and cultured in alpha modification of Eagle's medium (GIBCO BRL, Grand Island, NY) supplemented with 10% fetal bovine serum (GIBCO BRL), 100  $\mu$ M ascorbic acid 2-phosphate (Sigma Aldrich, St. Louis, MO), 2 mM glutamine, 100 U/mL penicillin, and 100  $\mu$ g/mL streptomycin (GIBCO BRL) (growth medium) and incubated at 37°C in 5% CO<sub>2</sub> (normoxia). All primary cells used in this study were passage 2 or 3 cells. Hypoxia was induced by exposure to a gas mixture of 8% O<sub>2</sub>, 5% CO<sub>2</sub>, and 85% N<sub>2</sub>. Hypoxyprobe™-1 kit (Hypoxyprobe, Inc., Burlington, MA) was used to detect the *in vitro* cellular response to hypoxia. Cells were incubated under hypoxia for 48 h in the presence of 200  $\mu$ M Hypoxyprobe™-1 followed by immunocytochemical staining. Cellular hypoxia was also confirmed by immunocytochemical staining of HIF-1 $\alpha$ .

### Flow cytometric analysis

To characterize the immunophenotype of human PDLSCs and PAFSCs, expression of mesenchymal stem cell (MSC)-associated surface markers at passage 3 was analyzed by flow cytometry as previously described.<sup>24</sup> Briefly, cells in their third passage ( $1.0 \times 10^6$  cells) were fixed with 4% PFA for 10 min and resuspended in 1% bovine serum albumin (BSA) phosphate-buffered saline (PBS) for blocking for 30 min. Cells were then incubated with specific antibodies for CD13 (0.1  $\mu$ g/mL), CD34 (0.1  $\mu$ g/mL), CD90 (0.05  $\mu$ g/mL), or CD146 (0.1  $\mu$ g/mL) at 4°C for 1 h, followed by the addition of fluorescently labeled secondary antibodies at room temperature for 1 h. All antibodies were purchased from BD Biosciences (San Jose, CA). The percentage of CD13-, CD90-, and CD146-positive and CD34-negative cells was measured with an FACS Calibur (Becton Dickinson, CA), and the results were analyzed using Cell Quest Pro software (Becton Dickinson).

### Mineralization induction and Alizarin red S staining

For mineralization, cells were cultured in osteogenic medium (growth medium supplemented with 10 mM  $\beta$ -glycerophosphate, 50  $\mu$ g/mL ascorbic acid, and 100 nM dexamethasone) for 3 weeks. For undifferentiated samples, cells were maintained in growth medium for the same duration. Mineral nodule formation was observed by staining the cultures with 40 mM Alizarin red S (pH 4.2), and the amount of Alizarin red S that bound to the minerals in each dish was quantified by destaining the samples in 10 mM sodium phosphate containing 10% cetylpyridinium chloride (pH 7.0) for 15 min at room temperature. The amount of Alizarin red S in the destaining solution was measured at OD 562 nm and compared with a standard solution of the dye.<sup>25</sup>

### *Chondrogenic and adipogenic differentiation*

To induce chondrogenic or adipogenic differentiation, cells were cultured in StemPro Chondrogenic or StemPro Adipogenic differentiation media (GIBCO BRL), respectively, with appropriate supplements. At week 2 of post-chondrogenic or postadipogenic induction, cells were washed with PBS and fixed in 4% paraformaldehyde for 10 min. Cells were stained with 1% Alcian Blue (Sigma Aldrich) and 0.3% Oil Red O dye (Sigma Aldrich) to detect proteoglycans and fat vacuoles as an indication of chondrogenic and adipogenic differentiation, respectively. Cells were visualized under an inverted light microscope (Olympus U-SPT; Olympus, Tokyo, Japan).

### *Cell proliferation/cytotoxicity assay*

Cell proliferation was measured using the colorimetric 3-(4,5-dimethylthazol-2-yl)-2,5-diphenyltetrazolium bromide assay kit (Promega, Madison, WI). Briefly, human PDLSCs and PAFSCs ( $3.0 \times 10^3$  cells/well) were seeded in 96-well plates and cultured for 24 or 48 h. Cells were then exposed to 8% oxygen or chemicals, including DFO (Sigma Aldrich) or YC-1 (Sigma Aldrich) at various concentrations for the indicated durations. Fifteen microliters of premixed optimized dye solution was added 4 h before the treatment was stopped. Each condition was prepared in triplicate, and reactions were assessed using an ELISA reader at OD 595 nm (reference, 655 nm).

### *Western blot analysis*

Human PDLSCs and PAFSCs ( $1.0 \times 10^6$  cells/dish) were seeded in 100-mm culture dishes and cultured for various times. Protein concentrations of whole cell lysates were determined using a DC Protein Assay Kit (Bio-Rad Laboratories, Hercules, CA). Equal amounts of protein (30  $\mu$ g/lane) were resolved by 10% sodium dodecyl sulfate–polyacrylamide gel electrophoresis followed by transfer to a polyvinylidene difluoride membrane (GE Healthcare, Chalfont St. Giles, Buckinghamshire, United Kingdom). Specific antibodies against CEMP1 were produced as previously described.<sup>26</sup> Primary antibodies against hemagglutinin (HA; 0.01  $\mu$ g/mL) (Invitrogen, Carlsbad, CA), HIF-1 $\alpha$  (0.01  $\mu$ g/mL) (Epitomics, Burlingame, CA), and  $\beta$ -actin (Santa Cruz Biotechnology, Santa Cruz, CA) were used for blots that were finally developed using horseradish peroxidase-conjugated secondary antibodies (Santa Cruz Biotechnology) and visualized by enhanced chemiluminescence (enhanced chemiluminescence kit; GE Healthcare, Pittsburgh, PA).

### *Immunocytochemical staining*

Cells were fixed in 4% paraformaldehyde in PBS at room temperature for 10 min. After rinsing with PBS, cells were blocked with 5% BSA and 0.2% Tween-20 in PBS for 30 min at room temperature. Cells were then treated with primary antibodies for Hypoxyprobe-1 (pimonidazole) (0.05  $\mu$ g/mL), HIF-1 $\alpha$  (0.05  $\mu$ g/mL), or CEMP1 (0.5  $\mu$ g/mL) for 16 h at 4°C. Normal mouse, rabbit, or goat IgGs (Santa Cruz Biotechnology) for each primary antibody were used as controls. Alexa Fluor<sup>®</sup> dyes-conjugated second antibodies (Invitrogen) were used for double staining. DAPI was used for counter-

staining. Cell staining was evaluated using a fluorescence microscope (Olympus BX51; Olympus).

### *DNA constructs and transfection*

A full-length open reading frame of HIF-1 $\alpha$  (Accession No. NM\_010431) was cloned into the pENTR D-TOPO vector (Invitrogen). All expression constructs were modified to include the nine amino-acid HA epitope YPYDVPDYA fused directly to the C-terminus. For expression in cell culture, a derivative of the Piggybac transposon system that facilitates high efficiency expression was employed.<sup>27</sup> PBX2.2 empty vector and PBX2.1-EGFP for GFP expression were kindly provided by T. Sanders (University of California, San Francisco). Transfection experiments were performed with Lipofectamine LTX and PLUS reagent (Invitrogen). A 2:1 molar ratio of Piggybac transposase helper plasmid<sup>27</sup> was combined with the transposon expression construct to mediate integration and high levels of expression.

### *RNA interference*

At 24 h before transfection, cells were seeded onto a 24-well plate and grown to 60–70% confluence. Cells were transiently transfected with 20 nM HIF-1 $\alpha$  siRNA (Santa Cruz Biotechnology) and control siRNA (Santa Cruz Biotechnology) for 4 h using Lipofectamine<sup>™</sup> RNAiMAX reagent (Invitrogen) according to the manufacturer's instructions. After 48 h, transfected cells were harvested for RNA and whole cell lysate preparation.

### *Alkaline phosphatase assay and staining*

Quantitative alkaline phosphatase (ALP) activity was determined by an assay based on the hydrolysis of p-nitrophenylphosphate (p-NPP) to p-nitrophenol (p-NP). Human PAFSCs and PDLSCs cultured in induction media for 21 days were harvested in lysis buffer solution containing 0.1% Triton X-100. Cell lysates (60  $\mu$ L) from DSC samples were added to 60  $\mu$ L 0.2 M diethanolamine and 30 mM p-NPP. Samples were then incubated at 37°C for 30 min, and the reaction was stopped by the addition of 60  $\mu$ L 0.3 N sodium hydroxide. ALP activity was determined from the absorbance of p-NP at a wavelength of 410 nm using a microplate reader. For ALP staining, cells were fixed in 10% formalin, incubated with 0.1% Triton X-100 for 5 min, and then stained with the Leukocyte ALP kit (Sigma Aldrich) according to the manufacturer's protocol.

### *RNA preparation and real-time quantitative PCR analysis*

To evaluate gene expression levels in human PAFSCs and PDLSCs,  $5.0 \times 10^5$  cells were seeded in a 60 mm culture dish and cultured for 3 weeks under mineralization differentiation induction conditions. Total RNA was prepared using an RNeasy Mini kit (QIAGEN, Valencia, CA) according to the manufacturer's instructions, and cDNA was synthesized from 2  $\mu$ g of total RNA using Superscript II reverse transcriptase (Invitrogen). Real-time PCR was performed with SYBR Green PCR Master Mix (Applied Biosystems, Warrington, Cheshire, United Kingdom) by following the manufacturer's protocols. Reaction conditions comprised 40 cycles of 15 s of denaturation at 95°C and 1 min of amplification

at 60°C. All reactions were run in triplicate, and expression was normalized to that of the housekeeping gene *glyceraldehyde-3-phosphate dehydrogenase (Gapdh)*. Relative levels of transcript expression were quantified using the  $\Delta\Delta Ct$  method.<sup>28</sup> The calculation was performed by using the *Ct* value of *Gapdh* to normalize the *Ct* value of the target gene in each sample to obtain the  $\Delta Ct$  value, which was then used to compare different samples. Relative mRNA expression was compared in a histogram. Specific primers sets used in the analysis are listed in Table 1.

#### In vivo experiments

**Animals.** All animal-use procedures and experimental protocols were conducted according to the guidelines of the institutional animal care and use committee (No. SNU – 120427-2, ilar.snu.ac.kr, IACUC) at Seoul National University. ICR mice were obtained from Orientbio, Inc. (Sungnam, Korea) and maintained on a daily feed of rodent food in housing quarters with regulated temperature, cycled light (12 h on/off), and sterile water.

**Detection of tissue hypoxia.** To detect mouse tissue hypoxia, we employed the Hypoxyprobe™-1 kit that contains pimonidazole hydrochloride and detection antibodies (Hypoxyprobe, Inc., Burlington, MA). Pimonidazole was injected intraperitoneally on postnatal days 7 and 14 in ICR mice (60 mg/kg) 90 min before sacrifice ( $n=3$ ). Tissue fixation was performed by *in vivo* perfusion to eliminate artificial staining.<sup>29</sup> All animals were anesthetized with a mixture of ketamine HCL (Parke-Davis, Morris Plains, NJ) plus 20% xylazine I.P. (Moby Corporation, Shawnee, KS) and perfused with 0.1 M PBS (pH 7.4) for 30 s and then 4% PFA solution through the left ventricle for 5 min (5 mL/min) using a three-way stopcock that enabled the operator to quickly switch from rinsing to fixation solution, thus avoiding a drop in perfusion pressure. After tissue preparation, immunohistochemistry (IHC) was performed to detect tissue hypoxia using antibodies included in the Hypoxyprobe™-1 kit.

**In vivo DFO treatment.** To study the effects of DFO on cementum formation during tooth developmental stages *in vivo*, we divided ICR mice into two groups: a DFO group ( $n=6$ ); 25 mg/kg/day of DFO was injected intraperitoneally

everyday from postnatal days 7 to 13, and a control group ( $n=6$ ); the same volume of saline was injected at the same time points as used for the DFO group. Mice from each group were sacrificed at postnatal day 14 for histological analysis.

**Tissue preparation and IHC.** Whole murine heads were divided into two pieces by cutting the cranial sagittal suture, then fixed in 4% PFA solution for 48 h at 4°C, and decalcified with 12% EDTA for 21 days. After paraffin embedding, sections were cut serially in the sagittal plane from the most lingual side. During sectioning, the mid-sagittal plane of the tooth germ (P7) was defined as the plane where the highest point of the crown and the most middle portion of the pulp chamber appeared at the same time. Semi-serial 5  $\mu$ m sections of first and second molars were prepared and stained with hematoxylin and eosin (H&E) and IHC technologies. Primary antibodies for Hypoxyprobe-1 (pimonidazole) (0.05  $\mu$ g/mL), HIF-1 $\alpha$  (0.05  $\mu$ g/mL), bone sialoprotein (BSP; Santa Cruz Biotechnology) (0.05  $\mu$ g/mL), or CEMP1 (0.5  $\mu$ g/mL) were applied to paraffin-embedded tissue sections. Deparaffinized sections were immersed in 0.6% H<sub>2</sub>O<sub>2</sub>/methanol for 20 min to quench endogenous peroxidase activity. Sections were then incubated in 5% BSA in PBS for 30 min and incubated overnight at 4°C with each antibody (1:100). Sections were incubated for 1 h at room temperature with the secondary antibody and reacted with avidin-biotin-peroxidase complexes (Vector Laboratories, Burlingame, CA) in PBS for 30 min. After color development with 0.05% 3,3'-diaminobenzidine tetrahydrochloride (Vector Laboratories), sections were counterstained with hematoxylin. For Hypoxyprobe-1 staining, Alexa Fluor dye-conjugated secondary antibodies (Invitrogen) were used for double staining, and DAPI was used for counterstaining.

#### Statistical analysis

Statistical analysis was performed using Statistical Package for Social Science 13.0 software (SPSS, Inc., Chicago, IL). Normal data with equal variance were analyzed using one-way analysis of variance with a Tukey procedure. Significance was defined as  $p \leq 0.05$ . Values in each graph represent mean  $\pm$  standard errors. All assays were performed at least thrice, and representative data were presented.

## Results

### Characterization of human DSCs and multipotential differentiation

International Society for Cellular Therapy (ISCT) has proposed a set of criteria for defining human MSCs,<sup>30</sup> and these minimum standards have been widely accepted. At passage 3, both human PAFSCs (Fig. 1A) and PDLSCs (Fig. 1B) were characterized by flow cytometry. The percentage of positive cells was determined by the relative intensity of antibody-binding cells. CD13, CD90, and CD146 were highly expressed, whereas CD34 was expressed at a low level in both stem cell types. ISCT has proposed that MSCs populations should be positive for CD90. In addition, these cells should exhibit low expression of hematopoietic antigens such as CD34 and markers for monocytes, macrophages, and B cells.<sup>30</sup> CD146 is

TABLE 1. PRIMER SEQUENCES FOR REAL-TIME QUANTITATIVE PCR

Gene	Accession No.	Sequences
<i>Cemp1</i>	AY584596	5'-AGAACCTCACCTGCCTCTCC-3' 5'-GATACCCACCTCTGCCTTGA-3'
<i>Ca IX</i>	NM_001216	5'-CACTCCTGCCCTCTGACTTC-3' 5'-AGAGGGTGTGGAGCTGCTTA-3'
<i>Ocn</i>	X53698	5'-GTGCAGAGTCCAGCAAAGGT-3' 5'-TCAGCCAACTCGTCACAGTC-3'
<i>Glut1</i>	AY034633	5'-CTTCACTGTCGTGTCGCTGT-3' 5'-CCAGGACCCACTTCAAAGAA-3'
<i>Gapdh</i>	NM_002046	5'-TCAAGAAGGTGGTGAAGCAG-3' 5'-AAAGGTGGAGGAGTGGGTGT-3'

*Ca IX*, carbonic anhydrase IX; *Gapdh*, glyceraldehyde-3-phosphate dehydrogenase; *Glut1*, Glucose transporter 1.

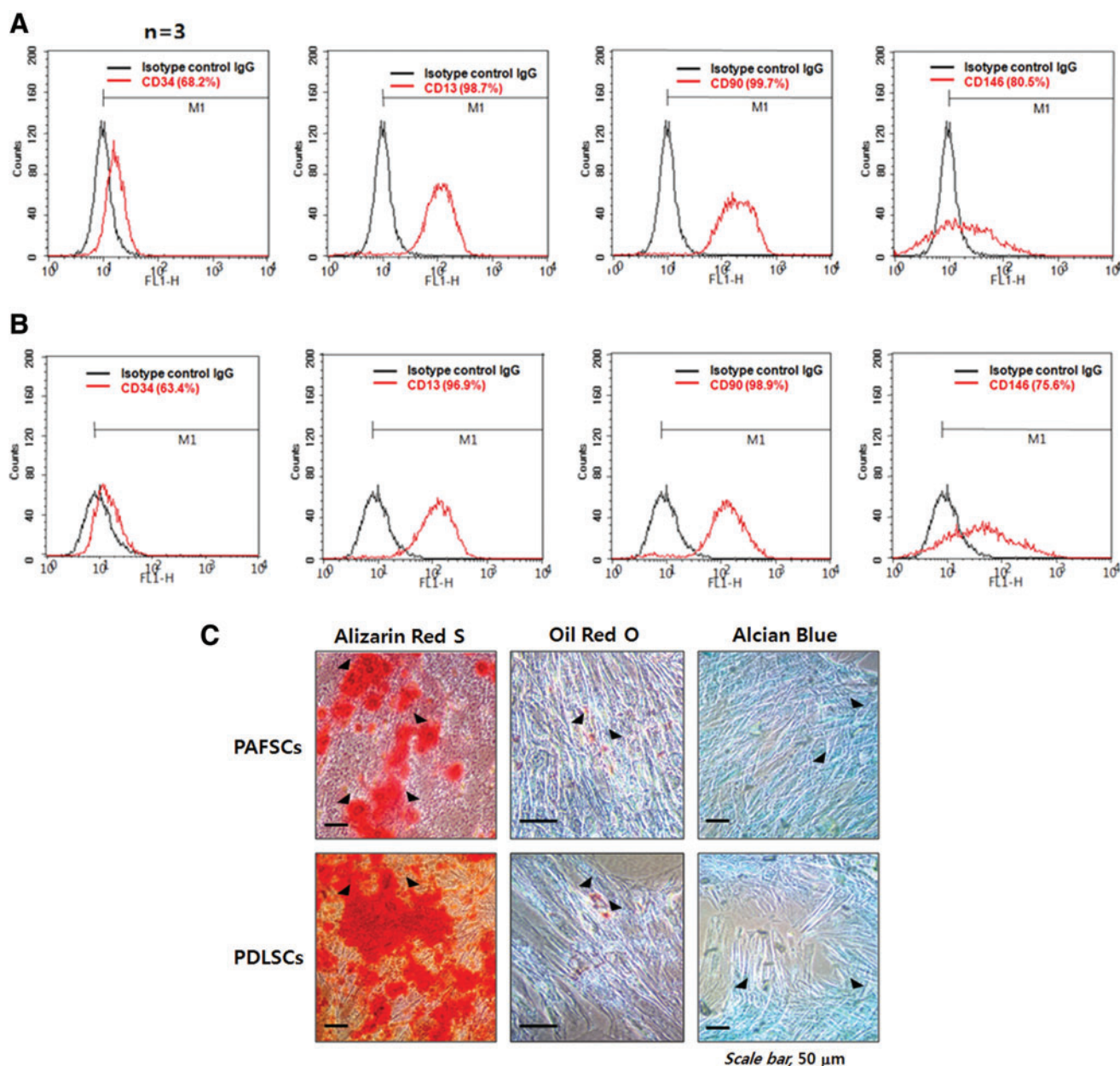


**FIG. 1.** Characterization of human dental stem cells by flow cytometric analysis and multipotential differentiation. Flow cytometry assays were performed with human PAFSCs (A) and PDLSCs (B) at passage 3. Expression levels of CD13, CD34, CD90, and CD146 were detected and expressed as a percentage for whole cells ( $n=3$ ). The percentage of isotypic control cells was deducted from that of the experimental cells at the right side of M1 gate. To investigate the differentiation potential of human PAFSCs and PDLSCs, cells were supplemented with osteogenic medium to induce mineralization *in vitro*. After 3 weeks of induction, cultured DSCs formed an extensive amount of Alizarin res S-positive mineral deposits (arrowheads) throughout adherent layers (C, left). Human PAFSCs and PDLSCs were also capable of undergoing adipogenic differentiation (arrow heads) in response to treatment with adipogenic-inductive supplements for 14 days (C, middle). Human PAFSCs and PDLSCs formed Alcian Blue-positive nodules (arrow heads) after 3 weeks of chondrogenic induction (C, right). DSCs, dental stem cells; PAFSCs, periapical follicular stem cells; PDLSCs, periodontal ligament stem cells. Color images available online at [www.liebertpub.com/tea](http://www.liebertpub.com/tea)

a representative putative MSC marker. Our results indicated that the isolated cells were mainly mesenchymal and minimally contaminated with epithelial cells. To investigate the multipotent differentiation potential of human PAFSCs and PDLSCs, cells were supplemented with osteogenic medium to induce mineralization *in vitro*. After 3 weeks of induction, cultured DSCs formed an extensive amount of Alizarin res

S-positive mineral deposits throughout adherent layers (Fig. 1C, left). Human PAFSCs and PDLSCs were also capable of undergoing adipogenic differentiation in response to treatment with adipogenic-inductive supplements for 14 days (Fig. 1C, middle). Moreover, human PAFSCs and PDLSCs formed Alcian Blue-positive nodules after 3 weeks of chondrogenic induction (Fig. 1C, right).

### Reduced oxygen tension stabilizes the HIF-1 $\alpha$ protein and induces proliferation of human PDLSCs *in vitro*

Our preliminary data showed that anoxia and severe hypoxia (<2% oxygen) increased cell death substantially. Although 8% is higher than usual hypoxia when compared with other experiments, it is closer to the physiological oxygen tension experienced by embryonic stem cells,<sup>10</sup> somatic stem cells,<sup>10,17</sup> and DSCs.<sup>31</sup> To confirm cellular hypoxia at 8% oxygen, we evaluated the accumulation of HIF-1 $\alpha$  protein *in vitro*. Hypoxic response in these cells is characterized by an increase in pimonidazole adducts that form a stable covalent bond with the thiol groups of proteins<sup>32</sup> as shown by immunocytochemical analysis (Fig. 2A). HIF-1 $\alpha$  protein expression in the nucleus of cells exposed to 8% oxygen for 24 h increased markedly. The hypoxic response in PDLSCs was similar to that in PAFSCs (data not shown). To examine the effect of the hypoxic state on cell viability, we performed cell proliferation assays. As shown in Figure 2B, PAFSCs and PDLSCs exposed to 8% oxygen proliferated to a greater extent (119.2% $\pm$ 19.6% and 132.8% $\pm$ 20.4%, respectively) than control cells.

### Hypoxia induces the expression of cementum-associated genes *in vitro*

To examine the hypothesis that cementoblast differentiation is regulated by oxygen tension, human PAFSCs and PDLSCs were cultured at 8% or 20% oxygen. To evaluate the activity of HIF-1 $\alpha$  as a functional transcription factor, the expression of HIF-1 $\alpha$  target genes was examined by real-time PCR in human PAFSCs (Fig. 3A) and PDLSCs (Fig. 3B) exposed to 8% oxygen. The expression of a HIF-1 $\alpha$  target gene, *carbonic anhydrase IX (Ca IX)*<sup>33</sup> was up-regulated by 1.2-fold and 2.9-fold in human PAFSCs and PDLSCs treated with 8% oxygen for 21 days, respectively. To examine the effect of hypoxia on the expression of the cementum-associated genes, namely *Cemp1* and *Ocn*,<sup>34</sup> we analyzed the expression level of those genes in human PAFSCs and PDLSCs after differentiation. *Cemp1* expression was dramatically up-regulated in human PAFSCs and PDLSCs treated with 8% oxygen for 21 days by 11.6-fold and 4.8-fold, respectively. The expression of *Ocn* was also up-regulated in human

PAFSCs and PDLSCs treated with 8% oxygen for 21 days by 5.6- and 5.2-fold, respectively. The expression of other cementum-associated genes, namely *protein-tyrosine phosphatase-like member-a cementum attachment protein (Ptpla-cap)*<sup>35</sup> and *F-spondin*,<sup>36</sup> was also examined *in vitro*; however, expression levels of these genes did not change significantly in response to oxygen treatment (data not shown).

### Hypoxia induces CEMP1 protein expression *in vitro*

Next, we evaluated the protein level of CEMP1 in human PAFSCs and PDLSCs differentiated in osteogenic medium for 21 days by western blot analysis (Fig. 3C). Intrinsic expression of CEMP1 protein was lower in undifferentiated PDLSCs (62.0% $\pm$ 3.9%) than in undifferentiated PAFSCs (Fig. 3C, D). However, CEMP1 protein expression in differentiated PDLSCs increased dramatically to 467.6% $\pm$ 8.0% relative to the undifferentiated control (Fig. 3C, E). CEMP1 protein expression in PAFSCs also increased in response to osteogenic differentiation to 137.2% $\pm$ 5.2%. When cells were treated with 8% oxygen, CEMP1 protein expression increased to 233.8% $\pm$ 46.2% in human PAFSCs and 110.5% $\pm$ 2.5% in PDLSCs (Fig. 3F). These data indicate that CEMP1 protein expression in both human PAFSCs and PDLSCs is significantly up-regulated when these cells are exposed to low oxygen tension during differentiation. Although CEMP1 protein induction in PAFSCs was more sensitive to hypoxia, CEMP1 induction was higher in PDLSCs than in PAFSCs, suggesting that the response of DSCs to hypoxia is cell-type specific.

### Hypoxia enhances mineralization and ALP activity *in vitro*

During 21 days of osteogenic differentiation, both PAFSCs and PDLSCs exposed to 8% oxygen showed higher mineralization than control cells as shown by Alizarin red S staining (Fig. 4A). Mineralization in human PAFSCs and PDLSCs treated with 8% oxygen increased to 116.3% $\pm$ 11.0% and 164.2% $\pm$ 4.5%, respectively (Fig. 4B). Furthermore, ALP activity in human PAFSCs and PDLSCs treated with 8% oxygen increased to 117.4% $\pm$ 1.5% and 127.8% $\pm$ 4.3%, respectively (Fig. 4C). Both human PAFSCs and PDLSCs

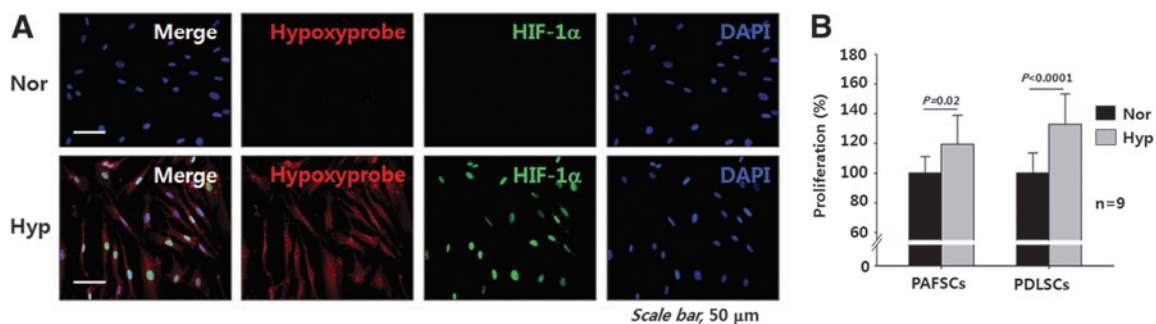


**FIG. 2.** Reduced oxygen tension (8%) induced cellular hypoxic response and proliferation *in vitro*. Immunocytochemical staining was performed to test the cellular hypoxia. Hypoxyprobe (pimonidazole adduct)-positive cells were strongly positive for nuclear HIF-1 $\alpha$  expression in PAFSCs exposed to 8% O<sub>2</sub> (Hyp) for 48 h compared with normoxia (Nor) control (A). Scale bar, 50  $\mu$ m. To examine the effect of hypoxia on cell proliferation of human PAFSCs and PDLSCs *in vitro*, cell proliferation assay was performed and expressed as a percentage for its normoxia control (B). The statistical *p*-values of the intergroup were analyzed by ANOVA followed by Tukey test for direct pair-wise comparisons and indicated in the graph (*n*=9). ANOVA, analysis of variance; HIF, hypoxia-inducible factor.

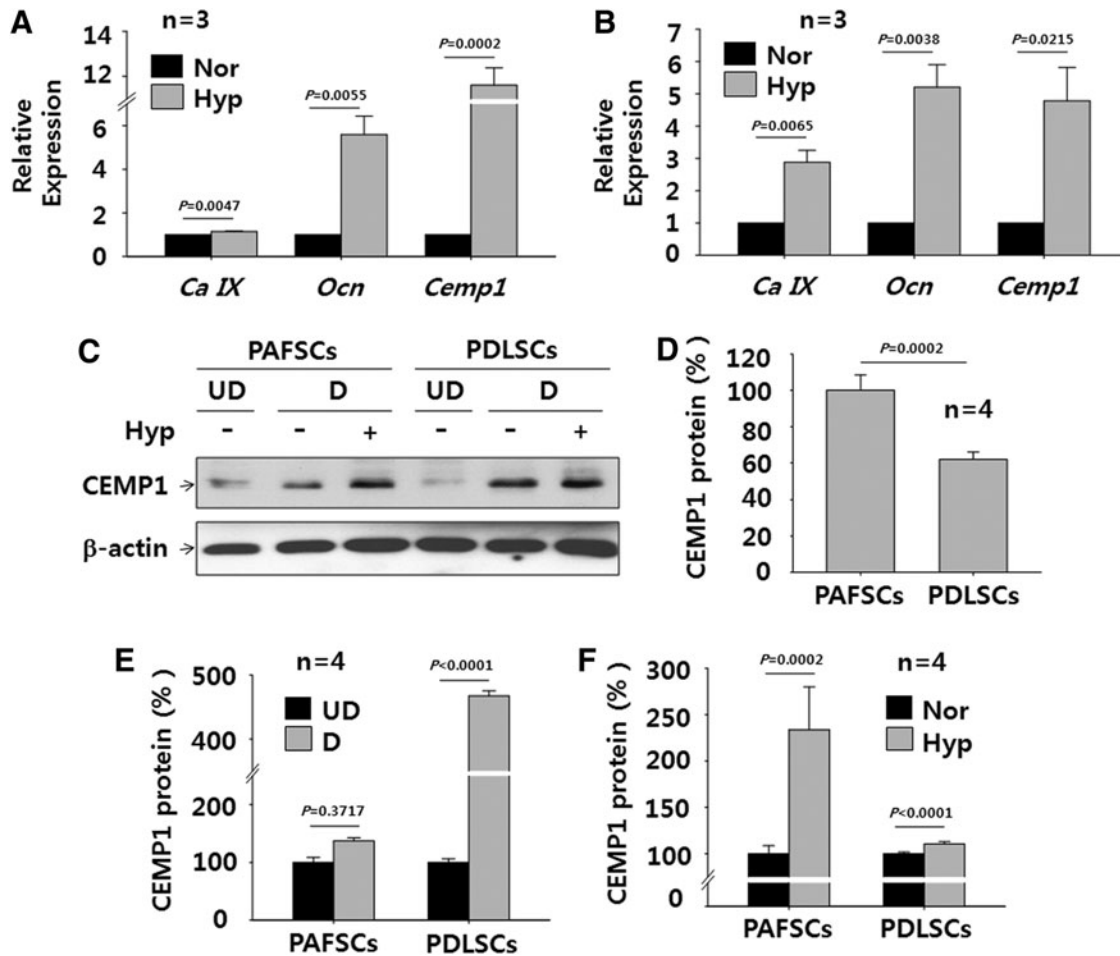


**FIG. 3.** Hypoxia induces the expression of cementum-associated genes and CEMP1 protein *in vitro*. To examine the effect of hypoxia on differentiation into cementoblast-like cells, quantitative real-time PCR was performed after differentiation for 21 days in human PAFSCs (**A**) and PDLSCs (**B**). The expression of *Cemp1* and *Ocn* was induced by hypoxia in both cells, and *Ca IX* was used as a target of HIF-1 $\alpha$ . To evaluate cellular CEMP1 protein level, Western blot assay was performed (**C**). Densitometric analysis was performed to compare CEMP1 protein level as follows: Intrinsic CEMP1 protein levels between human PAFSCs and PDLSCs were compared (**D**). After osteogenic differentiation, CEMP1 protein levels of both cells between undifferentiated (UD) and differentiated (D) states were also compared (**E**). Finally, CEMP1 protein levels of both differentiated cells in a hypoxic culture condition were compared with those of normoxic control (**F**). The statistical *p*-values of the intergroup were analyzed by ANOVA followed by Tukey test for direct pair-wise comparisons and indicated in the graph ( $n \geq 3$ ). *Ca IX*, carbonic anhydrase IX; CEMP1, cementum protein 1.

treated with 8% oxygen also showed increased ALP protein staining (Fig. 4D).

#### Pharmacological activation of the HIF-1 pathway induces CEMP1 expression *in vitro*

A family of oxygen-sensitive prolyl hydroxylases (PHDs) hydroxylate HIFs under normoxia, which promotes their subsequent E-3 ligation and proteosomal destruction.<sup>37</sup> To differentiate between an increase in HIF-1 $\alpha$  and other effects of a low oxygen environment, we blocked HIF-1 $\alpha$  degradation with DFO, a known PHDs inhibitor, to activate the HIF-1 pathway at 20% oxygen. The optimum level of DFO was determined based on cytotoxicity analysis in both cell types (Supplementary Fig. S2). Minimum cytotoxicity in PDLSCs was observed at 1  $\mu$ M DFO ( $94.6\% \pm 12.4\%$  proliferation), but maximum mineralization was observed. DFO treatment of both PAFSCs and PDLSCs for 24 h at 20% oxygen increased

HIF-1 $\alpha$  and CEMP1 protein expression to levels similar to those observed for hypoxia (Fig. 5A). In addition, Alizarin red S staining showed that mineralization was also induced in PDLSCs treated with DFO at 20% oxygen (Fig. 5B) as well as in PAFSCs (data not shown).

#### Enforced expression of HIF-1 $\alpha$ enhances CEMP1 expression *in vitro*

Next, we introduced HIF-1 $\alpha$  into the cells to investigate the effect of HIF-1 on CEMP1 protein expression and then performed real-time PCR and western blot analysis. As expected, HIF-1 $\alpha$  up-regulated the expression of *Cemp1* (Fig. 5C) as well as *Ca IX* and *Glucose transporter 1 (Glut1)*, which are known HIFs-target genes. In addition, CEMP1 protein expression in PDLSCs transfected with a plasmid harboring HIF-1 $\alpha$  fused with an HA tag (Fig. 5D) was confirmed by western blot analysis. Moreover, immunocytochemical

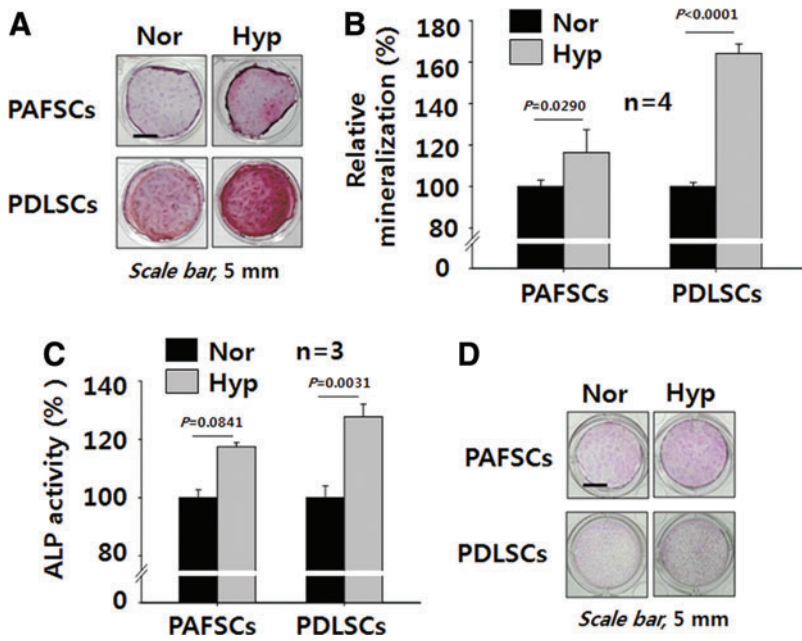


FIG. 4. Hypoxia enhances mineralization and ALP activity *in vitro*. Mineralization levels of human PAFSCs and PDLSCs differentiated under hypoxia for 21 days were evaluated by Alizarin red S staining and compared with their normoxia control (A, B). Relative mineralization (B) and ALP activity (C) were expressed as a percentage for their normoxic control. ALP levels of both cells were also analyzed by using cell lysate and ALP staining kit (D). The statistical *p*-values of the intergroup were analyzed by ANOVA followed by Tukey test for direct pair-wise comparisons and indicated in the graph ( $n=9$ ). Scale bar, 5 mm. ALP, alkaline phosphatase. Color images available online at [www.liebertpub.com/tea](http://www.liebertpub.com/tea)

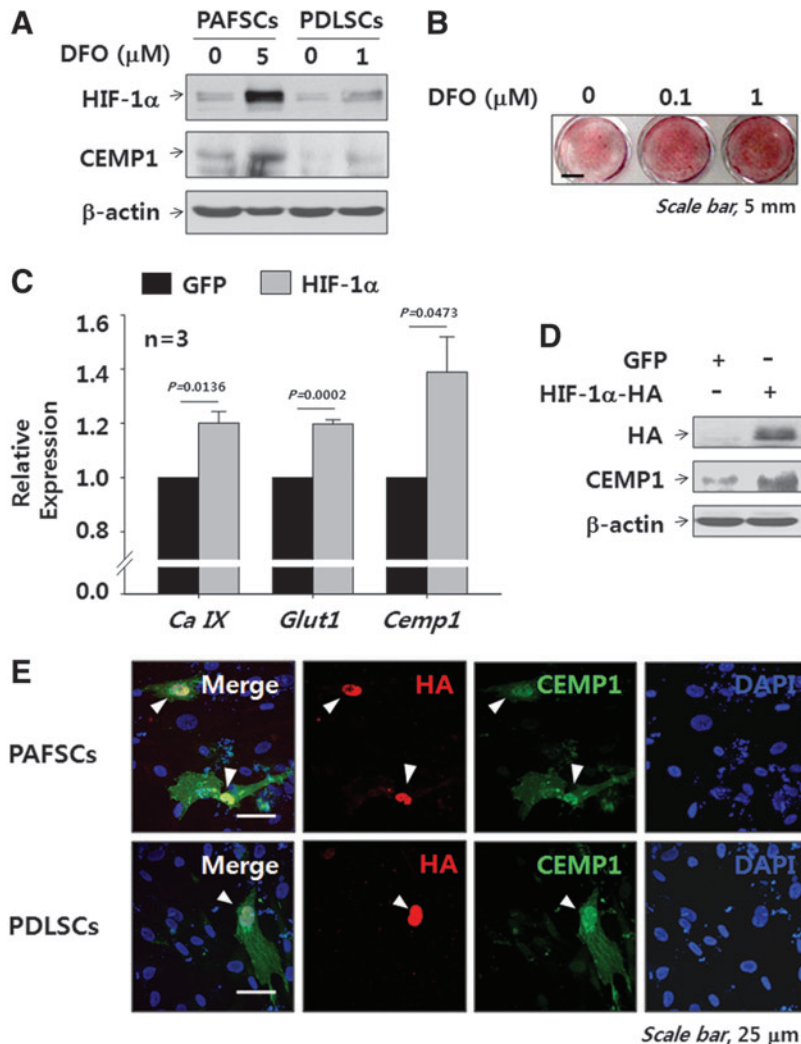


FIG. 5. Pharmacological and genetic activation of the HIF-1 $\alpha$  increases CEMP1 expression and final mineralization *in vitro*. Human PAFSCs and PDLSCs were treated with DFO for 24 h, and Western blot was performed to analyze the level of HIF-1 $\alpha$  and CEMP1 protein by using cell lysate (A). Human PDLSCs were differentiated with DFO treatment for 21 days and stained with Alizarin red S (B). Scale bar, 5 mm. Human PDLSCs were also transfected with HIF-1 $\alpha$ -HA and GFP constructs. GFP constructs were used as a control. Quantitative real-time PCR was performed after transfection for 24 h in human PDLSCs (C). *Ca IX* and *Glut1* were used as known targets of HIF-1 $\alpha$ . The statistical *p*-values of the intergroup were analyzed by ANOVA followed by Tukey test for direct pair-wise comparisons and indicated in the graph ( $n=3$ ). Western blot assay was also performed to analyze the level of HIF-1 $\alpha$  and CEMP1 protein by using cell lysate after transfection of human PDLSCs with HIF-1 $\alpha$ -HA and GFP constructs for 24 h (D). Immunocytochemical analysis of human PAFSCs and PDLSCs was performed to detect HA and CEMP1 protein (white arrowheads) after transfection of HIF-1 $\alpha$ -HA construct (E). Scale bar, 25  $\mu$ m. DFO, desferrioxamine; *Glut1*, *Glucose transporter 1*; HA, hemagglutinin. Color images available online at [www.liebertpub.com/tea](http://www.liebertpub.com/tea)



images clearly showed correlated expression of HIF-1 $\alpha$  and CEMP1 in PAFSCs and PDLSCs transfected with *Hif-1 $\alpha$*  (Fig. 5E).

#### *Inhibition of HIF-1 activity reduces CEMP1 protein expression and further mineralization in vitro*

To determine whether HIF-1 is responsible for induction of the CEMP1 protein and mineralization, we suppressed HIF-1 $\alpha$  expression by siRNA technology. The marked decrease in HIF-1 $\alpha$  protein expression at 8% O<sub>2</sub> indicates effective suppression of HIF-1 activity. CEMP1 protein expression was significantly lower at 8% oxygen in cells transfected with HIF-1 $\alpha$  siRNA than in cells transfected with control siRNA (Fig. 6A). In addition, we treated cells with YC-1, a potent HIF-1 inhibitor, to investigate whether HIF-1 inhibition reduced mineralization. The optimum level of YC-1 was determined by cytotoxicity analysis in both cell types (Supplementary Fig. S3). One micromolar YC-1 was not cytotoxic to either PAFSCs or PDLSCs; the proliferation rates of these two cell types were 131.8% $\pm$ 16.4% and 110.9% $\pm$ 11.0%, respectively. As expected, mineralization of PDLSCs treated with YC-1 at 8% oxygen for 21 days decreased significantly (Fig. 6B); the same effect was observed in PAFSCs (data not shown).

#### *Mouse tooth roots at postnatal day 7 develop in a hypoxic environment in the presence of CEMP1*

To assess the role of tissue hypoxia in mouse tooth development, we employed the hypoxia marker Hypoxyprobe-1, (pimonidazole hydrochloride).<sup>38</sup> Hypoxyprobe-1 is converted by hypoxia-activated nitroreductases into a reactive intermediate that forms covalent pimonidazole adducts with cellular components in hypoxic regions.<sup>29</sup> To detect tissue hypoxia in developing mouse tooth germ, mid-sagittal sections of the mandibular second molars were analyzed by IHC. As seen in Figure 7C, Hypoxyprobe-1 was highly concentrated at the proliferative root apex of the tooth germ at postnatal day 7, suggesting that highly proliferative cells may be localized to this region and contribute to local low oxygen tension. Pimonidazole adducts were highly concentrated at the apical area of the root edge and the central apex of the outer face of molar roots (Fig. 7F) when compared

with the vehicle-injected control (Fig. 7B, E). Of note, the cytoplasm of odontoblasts, which are typically arranged similar to a palisade along the pulp, was highly positive for Hypoxyprobe-1 at the apical area. However, the dental follicle (DF) surrounding the tooth germ appeared to remain non-hypoxic at this stage, while predentin exhibited weak nonspecific staining (asterisks in Fig. 7B, C). CEMP1 expression was highly correlated with tissue hypoxia as assessed by Hypoxyprobe-1 staining (Fig. 7I) and HIF-1 $\alpha$  measurement (Fig. 7H), suggesting that hypoxia may influence overall root development of mouse molars as well as CEMP1 expression to regulate cementum formation *in vivo*. The CEMP1 protein of mouse tooth germ at postnatal day 7 was immunolocalized in the DF and dental papilla at the apical area of root edge and the central apex in the outer face of molar roots and some of the pulp cells (Fig. 7F), while that of human adult tissue localized primarily to a restricted area of the PDL space (Supplementary Fig. S1).

#### *Mouse PDL space is hypoxic after tooth root formation in vivo*

To investigate tissue hypoxia in late tooth root development, we injected Hypoxyprobe-1 into mice at postnatal day 14 and fixed the tissue using an *in vivo* perfusion method to eliminate artificial staining. Days were selected to capture developmental time points of interest during tooth-bone interface development, including cementogenesis.<sup>21</sup> At postnatal day 14, root morphogenesis was almost finished and the root surface was covered with thin acellular cementum to facilitate attachment of the PDL.<sup>39</sup> At this stage, tissue hypoxia was localized mainly to the apical part of the PDL space and the furcation of molar roots (Figs. 8B, E, H) when compared with the vehicle-injected control (Figs. 8A, D, G). IHC revealed that most CEMP1-positive cells were localized to the PDL space at the furcation (Fig. 8F) and the apex (Fig. 8I) of molar roots.

#### *Stimulation of the HIF pathway enhances acellular cementogenesis in vivo*

To examine whether a similar pathway is involved in acellular cementum formation, we analyzed the cervical area of molar roots at postnatal 14 days. Using a refined IHC

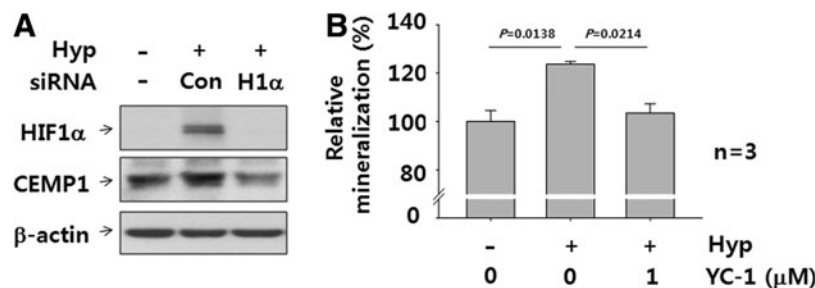


**FIG. 6.** RNA interference and pharmacological inhibition of the HIF-1 $\alpha$  decreases CEMP1 expression and mineralization *in vitro*. Human PDLSCs were transfected with HIF-1 $\alpha$  (H1 $\alpha$ ) and control (Con) siRNA for 24 h while exposed to hypoxia. Western blot was performed to analyze HIF-1 $\alpha$  and CEMP1 protein by using cell lysate and compared with control siRNA group (Con) (A). Human PDLSCs were differentiated with YC-1 treatment for 21 days, and mineralization was quantitated after Alizarin red S staining (B). Relative mineralization was expressed as a percentage for the control group. The statistical *p*-values of the intergroup were analyzed by ANOVA followed by Tukey test for direct pair-wise comparisons and indicated in the graph (*n* = 3).

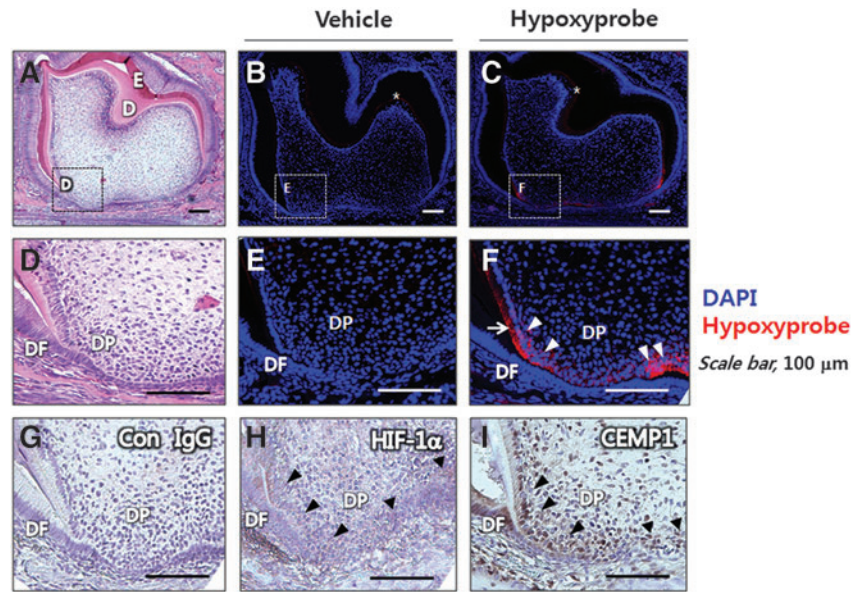


**FIG. 7.** Mouse tooth roots develop in hypoxic environment with CEMP1 expression at postnatal day 7 *in vivo*. An H&E staining section shows a whole tooth germ of the second lower molar at postnatal day 7 (A), and higher magnified H&E figures (black-dotted square) were also shown (D). To assess mouse tissue hypoxia, Hypoxyprobe-1 was injected intraperitoneally into ICR mouse at postnatal 7 days ( $n=3$ ) and analyzed by immunohistochemical staining (B, C, E-I) after tissue preparation. Analyzed with a magnified image, pimonidazole adducts were highly concentrated at the apical area of root edge and the central apex in the outer face of molar roots (white arrow head in F). Odontoblasts are typically palisade arranged along the pulp and have polarized cytoplasm with low oxygen tension (white arrow in F). Dental follicle (DF) surrounding tooth germ appeared to stay non-hypoxic at this stage, while predentin exhibited weak nonspecific staining (white asterisks in B, C). Immunohistochemical staining of developing mouse tooth germs at postnatal day 7 of the second lower molar was performed to localize HIF-1 $\alpha$  and CEMP1 protein and exhibited intense staining of Hypoxyprobe-1, HIF-1 $\alpha$ , and CEMP1 at the outer side of the growing root apex of a molar at postnatal day 7 (F, H, I, respectively). Control IgG (Con IgG) was used as a control for CEMP1 and HIF-1 $\alpha$  staining (G). E, enamel; D, dentin; DP, dental papilla. Scale bar, 100  $\mu$ m. H&E, hematoxylin and eosin.

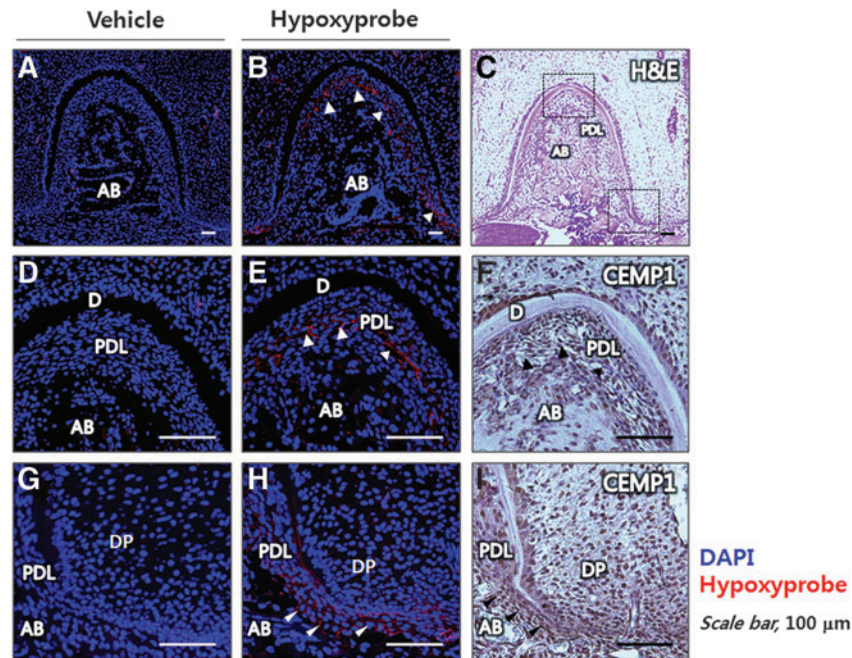


**FIG. 8.** Mouse PDL spaces are hypoxic at the formation of the tooth-bone interface *in vivo*. To assess mouse tissue hypoxia of developing mouse tooth root, Hypoxyprobe-1 was injected intraperitoneally into ICR mouse at postnatal day 14 ( $n=3$ ) and analyzed by immunohistochemical staining (A, B, D, E, G, H) after tissue preparation. An H&E staining section shows a whole tooth of the first lower molar in this stage (C). Tooth-bone interfaces (dotted squares) were magnified (E, H) and compared with vehicle-injected control (D, G). At this stage, tissue hypoxia was localized mainly to the PDL space at the furcation (white arrow heads in B, E) and the apical part (white arrow heads in B, H) of the molar root, when compared with vehicle-injected control (D, G). Immunohistochemical analysis shows that major CEMP1-positive cells are localized to the PDL space at the furcation (black arrow heads in F) and the apex (black arrow heads in I) of the molar roots. Immunolocalization of CEMP1 protein in these hypoxic regions was also performed with anti-CEMP1 antibody (F, I). D, dentin; AB, alveolar bone; PDL, periodontal ligament; DP, dental papilla. Scale bar, 100  $\mu$ m.

technique, which allows more sensitive identification of differential pimonidazole adducts, we discovered that tissue hypoxia localized differentially to the line covering the cervical cementum area (Figs. 9A–C, note the arrowhead in 9B) when compared with the vehicle-injected control (data not shown). Interestingly, the pimonidazole adduct-positive line colocalized with BSP (Fig. 9K), which is a mineral-binding member of the SIBLING family with a role in the mineralization process<sup>40</sup>; there is a close relationship between AEFC formation and the act of mineralization. To activate the HIF-1 pathway during tooth root development, we injected DFO daily into mice from postnatal day 7 to postnatal day 13. No significant differences in the general state of animals, including body weight or body temperature, were detected among groups during DFO injection. After 7 days of treating mice with DFO, there was a marked increase in pimonidazole adduct accumulation (Fig. 9E–G, note the arrowhead in 9F) and HIF-1 $\alpha$  protein expression (Fig. 9M) in PDL cells lining the cervical acellular cementum of mouse molar roots. CEMP1 was widely expressed during molar root formation and was expressed more strongly in the PDL space in response to DFO treatment than in the control (Fig. 9L). Despite increased expression of CEMP1 and HIF-1 $\alpha$  in the PDL space, overall cementum thickness did not change significantly as shown by immunolocalization of BSP (Fig. 9N). These results indicate that activation of the HIF-1 pathway induces CEMP1 protein expression and may affect cementogenesis during tooth root development *in vivo*.

## Discussion

CEMP1 was recently identified and characterized as a protein participating in biomineralization of progenitor cells in the PDL.<sup>9</sup> The precise mechanisms which couple CEMP1 expression to cementum formation are still unknown, but it appears that CEMP1-positive progenitor cells localized in the PDL participate in mineralization and differentiation of progenitor cells for cementum formation.<sup>8,41</sup> Indeed, previous studies showed that CEMP1 protein expression localized to the cementoblast cell layer lining the cementoid surface of cementum in both acellular and cellular cementum of human adult periodontal tissues.<sup>6,42</sup> Our immunohistochemical staining for CEMP1 in human tissues confirm these previous findings (Supplementary Fig. S1).

There are abundant reports that hypoxia induces proliferation of human MSCs.<sup>15,19,43</sup> It has also been reported that low oxygen tension during tissue culture has positive effects on mineralization and vascularization of bone.<sup>15–17,19,44</sup> However, the effects of hypoxia on osteogenesis and mineralization are still controversial.<sup>15,45–48</sup> Previous *in vitro* hypoxia experiments have been performed at lower oxygen tension (<2%) than the average physiological oxygen tension (4–8%).<sup>49</sup> Under low oxygen tension, bone marrow-derived MSCs show a decrease in osteogenic differentiation or spontaneous calcification.<sup>46–48</sup> Our preliminary oxygen gradient data indicate that neither PAFSCs nor PDLSCs were able to proliferate or undergo osteogenesis under 1% oxygen tension *in vitro* (data not shown). To mimic physiological oxygen conditions more closely, we subjected cells to 8% oxygen for long-term differentiation. Interestingly, hypoxia induced significant cementogenesis of human PAFSCs and PDLSCs at this oxygen tension. However, the responses of PAFSCs

and PDLSCs to hypoxia in terms of CEMP1 expression levels were different (Fig. 3F). Staining of human tissues for CEMP1 (Supplementary Fig. S1) indicated that PDLSCs could be a good source of progenitors for cementogenesis or regulation of cementogenesis, because PDLSCs expressed higher levels of CEMP1 protein during osteogenic differentiation than PAFSCs. Cells usually respond to external changes through crosstalk between cell surface proteins and cytoskeletal proteins. Therefore, cell surface molecules are likely to be involved in the differences in CEMP1 expression in the two cell types in response to hypoxia. The mechanisms underlying the difference in the expression of CEMP1 between PAFSCs and PDLSCs should be explored in future studies.

Our *in vivo* results indicate that oxygen tension was reduced by local proliferation of cells at the apical part of the tooth root during development (Fig. 7). At postnatal day 7, CEMP1 protein expression in the mouse tooth germ was highly correlated with tissue hypoxia. Interestingly, CEMP1 showed strong immunolocalization to the DF and dental papilla at the apical area of the root edge, the central apex in the outer face of molar roots, and some of the pulp cells (Fig. 7I), while human CEMP1 protein was localized to cementoblast cells and restricted PDL cell subpopulations (cementoblast precursors) in the PDL space (Supplementary Fig. S1). In addition, we have found that PDLSCs and other DSCs, including PAFSCs and dental pulp stem cells, express CEMP1 protein without osteogenic differentiation (unpublished data). These data support the possibility that CEMP1 has other roles in other types of cells during tooth development.

HIFs activate genes that regulate cellular events, and hypoxia and HIFs are responsible for several aspects of developmental morphogenesis. To obtain mechanical insights into cementogenesis in response to hypoxia, we demonstrated that HIF-1 activation by gene introduction or pharmacological activation induced CEMP1 expression in human PAFSCs and PDLSCs. Furthermore, we found that HIF-2 $\alpha$  induced CEMP1 expression significantly. However, it is unclear whether the two HIF- $\alpha$  proteins have redundant roles in cementogenesis. In sum, our *in vitro* experiments employing DSCs provided a mechanistic platform for probing the proposed roles of hypoxia in cementoblast mineralization and gene expression according to HIF-1 expression.

A few studies have investigated the role of hypoxia in tooth development, including root formation and cementogenesis. Based on our *in vitro* findings, HIF-1 stimulates cementum-associated gene expression and mineralization. We examined whether hypoxia affects tooth root and periodontum development and whether an HIF-1-modulating drug enhanced CEMP1 expression and cementoblastic differentiation *in vivo*. At postnatal day 7, mouse molar tooth germs develop (late bell stage). Tissue staining indicated that there was proliferation of stem cells at the apical region, resulting in local hypoxic environment. At postnatal day 14, the number of hypoxic regions in the PDL space increased, suggesting that a rigid tooth-anchoring structure formed in the periodontal tissue between the tooth root and alveolar bone during this stage of mouse tooth development. Given that CEMP1-expressing cells could be a source of progenitors for cementoblasts or regulators of cementogenesis, the fact that CEMP1 expression and pimonidazole adducts had a

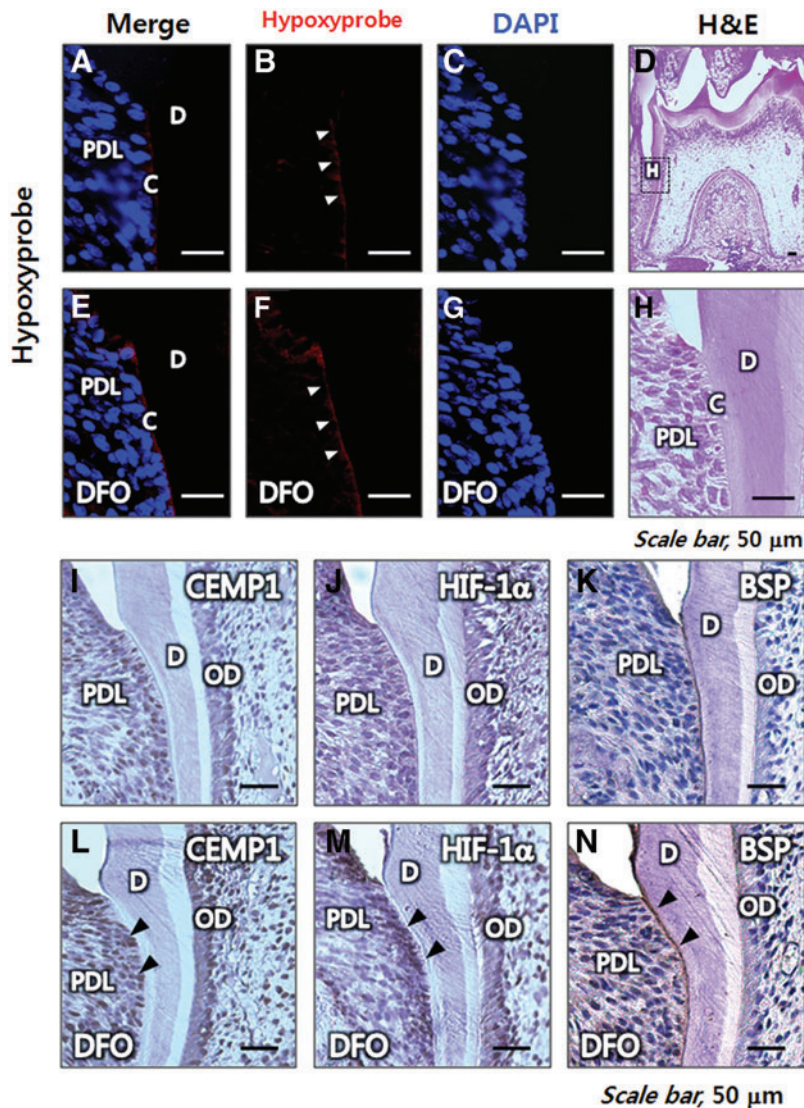


**FIG. 9.** Acellular cementogenesis occurs in a hypoxic environment, and stimulation of HIF pathway enhances acellular cementogenesis *in vivo*. Hypoxyprobe-1 was detected by immunohistochemical staining and analyzed to assess tissue hypoxia in cervical acellular cementum of mouse molar roots at the postnatal day 14. Hypoxyprobe-1 was also detected after DFO treatment to differentiate HIF-1 pathway in acellular cementum formation *in vivo* (E–G) and compared with untreated control (A–C). H&E image was shown to indicate the magnified area as well (D, H, respectively). Immunohistochemical staining shows that more CEMP1 (L) and HIF-1 $\alpha$ -positive PDL cells (M) were localized to the cervical cementum lining with DFX treatment when compared with control (I and J, respectively), and BSP expression was colocalized with this hypoxia-positive line at the cementum lining and was not changed with DFX treatment *in vivo* (N) when compared with control (K). C, cementum; D, dentin; OD, odontoblast; Scale bar, 50  $\mu$ m. BSP, bone sialoprotein. Color images available online at [www.liebertpub.com/tea](http://www.liebertpub.com/tea)

proximal distribution indicates that the hypoxic PDL space supports cementogenesis of progenitor cells by increased CEMP1 expression at the apical part and furcation of molar roots, corroborating our *in vitro* results. DFO is a metal-chelating drug that is often used in aluminum-overloaded patients who require dialysis. DFO can promote bone mineralization and regeneration without decreasing aluminum levels in the bone and have indirect effects on bone cells via HIF-1 $\alpha$  stabilization.<sup>50,51</sup> In this study, DFO induced a marked increase in CEMP1 and HIF-1 $\alpha$  protein expression in PDL cells *in vivo*. These findings strongly indicate that DFO may likewise regulate cementoblast differentiation of progenitor cells through the same pathway as osteoblast differentiation.

In summary, we demonstrated that hypoxia is accompanied by an increase in HIF-1 $\alpha$  protein expression, which, in turn, increases CEMP1 protein expression and mineralization of human DSCs such as PAFSCs and PDLSCs, promoting cementogenesis *in vitro*. We also provided evidence that HIF-1 activity is required to stimulate CEMP1 production and to allow mineralization and an ALP enzymatic response *in vitro*. Furthermore, we found that mouse tooth root development

occurs in a hypoxic state and that stimulation of the HIF-1 pathway enhances CEMP1 protein expression in mouse PDL spaces *in vivo*. Based on these findings, we suggest that the combination of hypoxia and human DSCs may be useful in regenerative therapies to repair periodontal defects.

#### Acknowledgment

This work was supported by a grant from the National Research Foundation of Korea (NRF) funded by the Korea government (MSIP) (No. 2011-0028922).

#### Disclosure Statement

No competing financial interests exist.

#### References

- Nanci, A., and Bosshardt, D.D. Structure of periodontal tissues in health and disease. *Periodontol* 2000 **40**, 11, 2006.
- Saygin, N.E., Giannobile, W.V., and Somerman, M.J. Molecular and cell biology of cementum. *Periodontol* 2000 **24**, 73, 2000.

3. Kitagawa, M., Tahara, H., Kitagawa, S., Oka, H., Kudo, Y., Sato, S., Ogawa, I., Miyaichi, M., and Takata, T. Characterization of established cementoblast-like cell lines from human cementum-lining cells *in vitro* and *in vivo*. *Bone* **39**, 1035, 2006.
4. Tobita, M., and Mizuno, H. Periodontal disease and periodontal tissue regeneration. *Curr Stem Cell Res Ther* **5**, 168, 2010.
5. Arzate, H., Jimenez-Garcia, L.F., Alvarez-Perez, M.A., Landa, A., Bar-Kana, I., and Pitaru, S. Immunolocalization of a human cementoblastoma-conditioned medium-derived protein. *J Dent Res* **81**, 541, 2002.
6. Alvarez-Perez, M.A., Narayanan, S., Zeichner-David, M., Rodriguez Carmona, B., and Arzate, H. Molecular cloning, expression and immunolocalization of a novel human cementum-derived protein (CP-23). *Bone* **38**, 409, 2006.
7. Alvarez Perez, M.A., Pitaru, S., Alvarez Fregoso, O., Reyes Gasga, J., and Arzate, H. Anti-cementoblastoma-derived protein antibody partially inhibits mineralization on a cementoblastic cell line. *J Struct Biol* **143**, 1, 2003.
8. Carmona-Rodriguez, B., Alvarez-Perez, M.A., Narayanan, A.S., Zeichner-David, M., Reyes-Gasga, J., Molina-Guarneros, J., Garcia-Hernandez, A.L., Suarez-Franco, J.L., Chavarria, I.G., Villarreal-Ramirez, E., and Arzate, H. Human Cementum Protein 1 induces expression of bone and cementum proteins by human gingival fibroblasts. *Biochem Biophys Res Commun* **358**, 763, 2007.
9. Villarreal-Ramirez, E., Moreno, A., Mas-Oliva, J., Chavez-Pacheco, J.L., Narayanan, A.S., Gil-Chavarria, I., Zeichner-David, M., and Arzate, H. Characterization of recombinant human cementum protein 1 (hrCEMP1): primary role in biomineralization. *Biochem Biophys Res Commun* **384**, 49, 2009.
10. Ezashi, T., Das, P., and Roberts, R.M. Low O<sub>2</sub> tensions and the prevention of differentiation of hES cells. *Proc Natl Acad Sci U S A* **102**, 4783, 2005.
11. Steinbrech, D.S., Longaker, M.T., Mehrara, B.J., Saadeh, P.B., Chin, G.S., Gerrets, R.P., Chau, D.C., Rowe, N.M., and Gittes, G.K. Fibroblast response to hypoxia: the relationship between angiogenesis and matrix regulation. *J Surg Res* **84**, 127, 1999.
12. Wang, D.W., Fermor, B., Gimble, J.M., Awad, H.A., and Guilak, F. Influence of oxygen on the proliferation and metabolism of adipose derived adult stem cells. *J Cell Physiol* **204**, 184, 2005.
13. Lennon, D.P., Edmison, J.M., and Caplan, A.I. Cultivation of rat marrow-derived mesenchymal stem cells in reduced oxygen tension: effects on *in vitro* and *in vivo* osteochondrogenesis. *J Cell Physiol* **187**, 345, 2001.
14. Horino, Y., Takahashi, S., Miura, T., and Takahashi, Y. Prolonged hypoxia accelerates the posttranscriptional process of collagen synthesis in cultured fibroblasts. *Life Sci* **71**, 3031, 2002.
15. Hung, S.P., Ho, J.H., Shih, Y.R., Lo, T., and Lee, O.K. Hypoxia promotes proliferation and osteogenic differentiation potentials of human mesenchymal stem cells. *J Orthop Res* **30**, 260, 2012.
16. Li, L., Zhu, Y.Q., Jiang, L., Peng, W., and Ritchie, H.H. Hypoxia promotes mineralization of human dental pulp cells. *J Endod* **37**, 799, 2011.
17. Grayson, W.L., Zhao, F., Izadpanah, R., Bunnell, B., and Ma, T. Effects of hypoxia on human mesenchymal stem cell expansion and plasticity in 3D constructs. *J Cell Physiol* **207**, 331, 2006.
18. Salim, A., Giaccia, A.J., and Longaker, M.T. Stem cell differentiation. *Nat Biotechnol* **22**, 804, 2004.
19. Grayson, W.L., Zhao, F., Bunnell, B., and Ma, T. Hypoxia enhances proliferation and tissue formation of human mesenchymal stem cells. *Biochem Biophys Res Commun* **358**, 948, 2007.
20. Semenza, G.L. Regulation of cancer cell metabolism by hypoxia-inducible factor 1. *Semin Cancer Biol* **19**, 12, 2009.
21. Huang, X., Bringas, P., Jr., Slavkin, H.C., and Chai, Y. Fate of HERS during tooth root development. *Dev Biol* **334**, 22, 2009.
22. Guo, W., Chen, L., Gong, K., Ding, B., Duan, Y., and Jin, Y. Heterogeneous dental follicle cells and the regeneration of complex periodontal tissues. *Tissue Eng Part A* **18**, 459, 2012.
23. Yang, Z., Jin, F., Zhang, X., Ma, D., Han, C., Huo, N., Wang, Y., Zhang, Y., Lin, Z., and Jin, Y. Tissue engineering of cementum/periodontal-ligament complex using a novel three-dimensional pellet cultivation system for human periodontal ligament stem cells. *Tissue Eng Part C Methods* **15**, 571, 2009.
24. Jin, H., Park, J.Y., Choi, H.J., and Choung, P.H. HDAC Inhibitor Trichostatin A promotes proliferation and odontoblast differentiation of human dental pulp stem cells. *Tissue Eng Part A* **19**, 613, 2013.
25. Jo, Y.Y., Lee, H.J., Kook, S.Y., Choung, H.W., Park, J.Y., Chung, J.H., Choung, Y.H., Kim, E.S., Yang, H.C., and Choung, P.H. Isolation and characterization of postnatal stem cells from human dental tissues. *Tissue Eng* **13**, 767, 2007.
26. Lee, D.S., Park, J.T., Kim, H.M., Ko, J.S., Son, H.H., Gronostajski, R.M., Cho, M.I., Choung, P.H., and Park, J.C. Nuclear factor I-C is essential for odontogenic cell proliferation and odontoblast differentiation during tooth root development. *J Biol Chem* **284**, 17293, 2009.
27. Yusa, K., Rad, R., Takeda, J., and Bradley, A. Generation of transgene-free induced pluripotent mouse stem cells by the piggyBac transposon. *Nat Methods* **6**, 363, 2009.
28. Livak, K.J., and Schmittgen, T.D. Analysis of relative gene expression data using real-time quantitative PCR and the 2(-Delta Delta C(T)) Method. *Methods* **25**, 402, 2001.
29. Rosenberger, C., Rosen, S., Paliege, A., and Heyman, S.N. Pimonidazole adduct immunohistochemistry in the rat kidney: detection of tissue hypoxia. *Methods Mol Biol* **466**, 161, 2009.
30. Dominici, M., Le Blanc, K., Mueller, I., Slaper-Cortenbach, I., Marini, F., Krause, D., Deans, R., Keating, A., Prockop, D., and Horwitz, E. Minimal criteria for defining multipotent mesenchymal stromal cells. The International Society for Cellular Therapy position statement. *Cytotherapy* **8**, 315, 2006.
31. Yu, C.Y., Boyd, N.M., Cringle, S.J., Alder, V.A., and Yu, D.Y. Oxygen distribution and consumption in rat lower incisor pulp. *Arch Oral Biol* **47**, 529, 2002.
32. Lee, Y.M., Jeong, C.H., Koo, S.Y., Son, M.J., Song, H.S., Bae, S.K., Raleigh, J.A., Chung, H.Y., Yoo, M.A., and Kim, K.W. Determination of hypoxic region by hypoxia marker in developing mouse embryos *in vivo*: a possible signal for vessel development. *Dev Dyn* **220**, 175, 2001.
33. Airley, R.E., Lancaster, J., Raleigh, J.A., Harris, A.L., Davidson, S.E., Hunter, R.D., West, C.M., and Stratford, I.J. GLUT-1 and CAIX as intrinsic markers of hypoxia in carcinoma of the cervix: relationship to pimonidazole binding. *Int J Cancer* **104**, 85, 2003.
34. Foster, B.L., Popowics, T.E., Fong, H.K., and Somerman, M.J. Advances in defining regulators of cementum development and periodontal regeneration. *Curr Top Dev Biol* **78**, 47, 2007.

35. Valdes De Hoyos, A., Hoz-Rodriguez, L., Arzate, H., and Narayanan, A.S. Isolation of protein-tyrosine phosphatase-like member-a variant from cementum. *J Dent Res* **91**, 203, 2012.
36. Kitagawa, M., Kudo, Y., Iizuka, S., Ogawa, I., Abiko, Y., Miyauchi, M., and Takata, T. Effect of F-spondin on cementoblastic differentiation of human periodontal ligament cells. *Biochem Biophys Res Commun* **349**, 1050, 2006.
37. Kaelin, W.G., Jr. The von Hippel-Lindau tumour suppressor protein: O<sub>2</sub> sensing and cancer. *Nat Rev Cancer* **8**, 865, 2008.
38. Varia, M.A., Calkins-Adams, D.P., Rinker, L.H., Kennedy, A.S., Novotny, D.B., Fowler, W.C., Jr., and Raleigh, J.A. Pimonidazole: a novel hypoxia marker for complementary study of tumor hypoxia and cell proliferation in cervical carcinoma. *Gynecol Oncol* **71**, 270, 1998.
39. Kim, T.H., Bae, C.H., Jang, E.H., Yoon, C.Y., Bae, Y., Ko, S.O., Taketo, M.M., and Cho, E.S. Col1a1-cre mediated activation of beta-catenin leads to aberrant dento-alveolar complex formation. *Anat Cell Biol* **45**, 193, 2012.
40. Fisher, L.W., and Fedarko, N.S. Six genes expressed in bones and teeth encode the current members of the SIBLING family of proteins. *Connect Tissue Res* **44 Suppl 1**, 33, 2003.
41. Komaki, M., Iwasaki, K., Arzate, H., Narayanan, A.S., Izumi, Y., and Morita, I. Cementum protein 1 (CEMP1) induces a cementoblastic phenotype and reduces osteoblastic differentiation in periodontal ligament cells. *J Cell Physiol* **227**, 649, 2012.
42. Park, J.Y., Jeon, S.H., and Choung, P.H. Efficacy of periodontal stem cell transplantation in the treatment of advanced periodontitis. *Cell Transplant* **20**, 271, 2011.
43. Sakdee, J.B., White, R.R., Pagonis, T.C., and Hauschka, P.V. Hypoxia-amplified proliferation of human dental pulp cells. *J Endod* **35**, 818, 2009.
44. Aranha, A.M., Zhang, Z., Neiva, K.G., Costa, C.A., Hebling, J., and Nor, J.E. Hypoxia enhances the angiogenic potential of human dental pulp cells. *J Endod* **36**, 1633, 2010.
45. Zahm, A.M., Bucaro, M.A., Srinivas, V., Shapiro, I.M., and Adams, C.S. Oxygen tension regulates preosteocyte maturation and mineralization. *Bone* **43**, 25, 2008.
46. Wang, Y., Li, J., Lei, L., Jiang, C., An, S., Zhan, Y., Cheng, Q., Zhao, Z., Wang, J., and Jiang, L. Effects of hypoxia on osteogenic differentiation of rat bone marrow mesenchymal stem cells. *Mol Cell Biochem* **362**, 25, 2012.
47. Huang, Y.C., Zhu, H.M., Cai, J.Q., Huang, Y.Z., Xu, J., Zhou, Y., Chen, X.H., Li, X.Q., Yang, Z.M., and Deng, L. Hypoxia inhibits the spontaneous calcification of bone marrow-derived mesenchymal stem cells. *J Cell Biochem* **113**, 1407, 2012.
48. Peterkova, R., Peterka, M., Viriot, L., and Lesot, H. Dentition development and budding morphogenesis. *J Craniofac Genet Dev Biol* **20**, 158, 2000.
49. Kofoed, H., Sjontoft, E., Siemssen, S.O., and Olesen, H.P. Bone marrow circulation after osteotomy. Blood flow, pO<sub>2</sub>, pCO<sub>2</sub>, and pressure studied in dogs. *Acta Orthop Scand* **56**, 400, 1985.
50. Wan, C., Gilbert, S.R., Wang, Y., Cao, X., Shen, X., Ramaswamy, G., Jacobsen, K.A., Alaql, Z.S., Eberhardt, A.W., Gerstenfeld, L.C., Einhorn, T.A., Deng, L., and Clemens, T.L. Activation of the hypoxia-inducible factor-1alpha pathway accelerates bone regeneration. *Proc Natl Acad Sci U S A* **105**, 686, 2008.
51. Qu, Z.H., Zhang, X.L., Tang, T.T., and Dai, K.R. Promotion of osteogenesis through beta-catenin signaling by desferrioxamine. *Biochem Biophys Res Commun* **370**, 332, 2008.

Address correspondence to:

Pill-Hoon Choung, DDS, PhD

Department of Oral and Maxillofacial Surgery

Dental Research Institute

School of Dentistry

Seoul National University

28 Yongon-dong

Chongno-gu

Seoul 110-749

Korea

E-mail: choungph@snu.ac.kr

Jong Hoon Chung, PhD

Department of Biosystems & Biomaterials

Science and Engineering

Seoul National University

599 Gwanangno

Gwanak-Gu

Seoul 151-921

Korea

E-mail: jchung@snu.ac.kr

Received: February 22, 2013

Accepted: August 26, 2013

Online Publication Date: December 13, 2013